

# From quantized states to percolation: Scanning tunneling spectroscopy of a strongly disordered two-dimensional electron system

J. Wiebe, Chr. Meyer, J. Klijn, M. Morgenstern, and R. Wiesendanger

*Institute of Applied Physics, Hamburg University, Jungiusstraße 11, D-20355 Hamburg, Germany*

(Received 10 April 2003; published 18 July 2003)

Low-temperature scanning tunneling spectroscopy is used to study the local density of states (LDOS) of an adsorbate induced two-dimensional electron system in a strong disorder potential. At low energy, completely confined states of s- and p-character are found in the valleys of the potential landscape. With increasing energy the whole area becomes filled with LDOS indicating percolation. The percolation threshold is marked by a significant decrease in the LDOS corrugation. Interestingly, we do not find a dominating wavelength in the Fourier transforms of the LDOS, suggesting that classical percolation is a reasonable concept to describe the transition.

DOI: 10.1103/PhysRevB.68.041402

PACS number(s): 73.21.Fg, 72.20.Ee, 71.55.Jv, 71.23.An

The concept of percolation is ubiquitous in solid state physics.<sup>1</sup> Recently, it has been proposed that percolation is responsible for the density-driven transition from metallic to insulating behavior in two-dimensional electron systems (2DESs),<sup>2</sup> that percolation could explain the doping dependence of transition temperatures in high- $T_c$  superconductors,<sup>3</sup> and that percolation might govern part of the complex phase diagram of the manganites.<sup>4</sup> However, the percolation transition of electron systems has barely been studied on the local scale. Here, we use a specifically prepared 2DES object to a relatively strong disorder potential to investigate the energy dependent transition from localized states to percolation on the nm scale. The system is the InAs inversion layer induced by small Co islands on the (110) surface.<sup>5</sup> Each island is at maximum singly charged, leading to a strongly fluctuating 2DES potential. At low energies, we observe single particle states confined in individual valleys of the potential landscape. These states exhibit lateral shapes as expected from s- and p-states. At higher energy, the local density of states (LDOS) becomes rather uniform and the corrugation strength drops from 90% to 45%, indicating percolation. Interestingly, we do not find an energy dependent dominating wave vector around the percolation threshold, which is in contrast to a 2DES investigated at much lower disorder.<sup>6</sup> Only the correlation function of the LDOS exhibits a small peak at the wavelength corresponding to the InAs dispersion. Thus, the system behaves rather classically and only a small remainder of a governing electron (Fermi) wavelength remains.

The ultrahigh vacuum low-temperature scanning tunneling microscope (STM) is described elsewhere.<sup>7</sup> It works at  $T=6$  K with an energy resolution of about 1 meV. PtIr-tips are prepared using standard techniques, and only tips which do not exhibit tip-induced quantum dot states<sup>8</sup> on the uncovered InAs(110) surface are used. To prepare the 2DES, we first cleave degenerate  $p$ -InAs ( $N_A=4.6\times 10^{17}/\text{cm}^3$ ) *in situ* at a base pressure of  $1\times 10^{-8}$  Pa. This results in a clean and mostly defect free InAs(110)-surface.<sup>9</sup> Then, Co is deposited by an  $e$ -beam evaporator to induce the inversion layer.<sup>5</sup> The Co coverage is calibrated by measuring the size of epitaxial Co islands on W(110). STM images are recorded in constant-

current mode with the voltage  $V$  applied to the sample. To obtain the LDOS, a differential conductivity map  $dI/dV(V,x,y)$  is recorded by a lock-in technique ( $V_{mod}=2-5$  mV).<sup>10</sup> Therefore, the tip is stabilized at a position  $(x,y)$ , voltage  $V_{stab}$  and current  $I_{stab}$  before  $dI/dV(V)$  is measured with  $V$  corresponding to the electron energy with respect to the Fermi level  $E_F$ .<sup>10</sup>

Figure 1(a) shows an STM image of the  $p$ -InAs(110) surface covered with  $5.5\times 10^{13}$  Co atoms/cm<sup>2</sup>. The Co forms islands visible as white bumps.<sup>5</sup> The island density is  $3.5\times 10^{12}$  cm<sup>-2</sup>, i.e., each island contains about 15 atoms. From previous photoemission experiments we know that such an island density transfers about  $2\times 10^{12}$  electrons/cm<sup>2</sup> to the sample, leading to a surface  $E_F$  shift of 500 meV.<sup>5</sup> Thus, about 50% of the Co islands are singly and positively

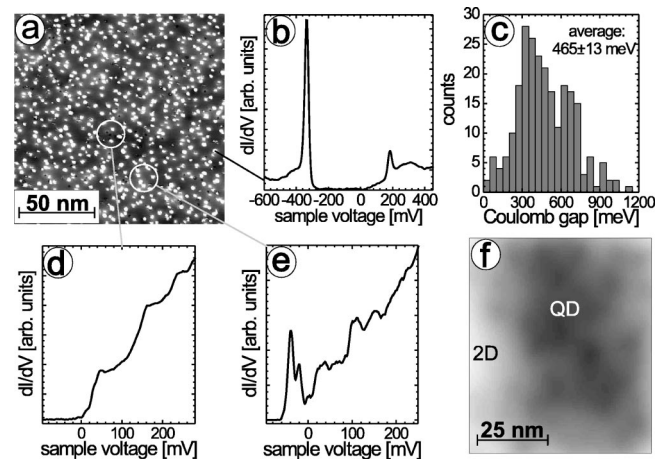


FIG. 1. (a) STM image of  $p$ -InAs(110) covered with 15% Co,  $V=500$  mV and  $I=500$  pA; circles and lines mark positions of spectra shown in (b), (d), and (e). (b)  $dI/dV$  curve taken on a Co cluster,  $I_{stab}=700$  pA,  $V_{stab}=700$  mV, and  $V_{mod}=5$  mV. (c) Histogram of obtained gap widths on different Co clusters. (d) and (e)  $dI/dV$  curves averaged over the circle regions marked in (a),  $I_{stab}=700$  pA,  $V_{stab}=500$  mV, and  $V_{mod}=5$  mV. (f) Potential landscape as deduced from the position of presumably charged clusters (see the text) (the gray scale covers 150 meV); the LDOS of this potential landscape is marked in Fig. 3; 2D and QD mark regions where  $dI/dV$  curves as in (d) and (e) are observed, respectively.

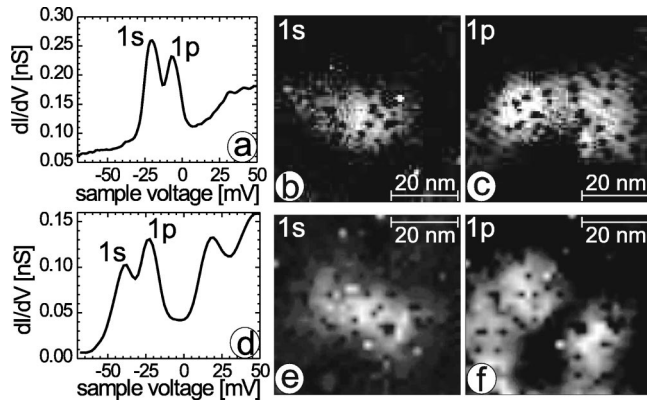


FIG. 2. (a)  $dI/dV$  curve from a region with two quantum dot states marked by  $1s$ ,  $1p$ ,  $I_{stab}=700$  pA,  $V_{stab}=500$  mV, and  $V_{mod}=5$  mV. (b) and (c)  $dI/dV$  images taken in the energy regions of the quantum dot peaks at  $V=-25$  ( $-16$ ) mV,  $I_{stab}=700$  pA,  $V_{stab}=430$  mV, and  $V_{mod}=2$  mV. (d) Same as (a) but for another region,  $I_{stab}=700$  pA,  $V_{stab}=430$  mV, and  $V_{mod}=5$  mV. (e) and (f)  $dI/dV$  images of peak regions,  $V=-40$  ( $-24$ ) mV,  $I_{stab}=700$  pA,  $V_{stab}=430$  mV, and  $V_{mod}=5$  mV; Co clusters appear as dark dots.

charged and a downward band bending on the InAs side results.

The Co islands can only be singly charged because of the strong Coulomb blockade within the islands. The Coulomb blockade becomes directly visible in  $dI/dV$  curves obtained on Co clusters. An example is shown in Fig. 1(b), where two peaks surround a region of zero conductivity. The position of the peaks, as well as the width of the gap, is different for each cluster. Gaps as large as 1.1 eV are observed. A histo-

gram of the gap widths is given in Fig. 1(c), revealing an average Coulomb gap of  $465 \pm 13$  meV. The averaged center of the Coulomb gaps is found at  $-140$  meV, which represents an average energy of the cluster ensemble, namely, the mean of the ionization energy and electron affinity. More importantly, the mean square width of the gap center distribution is as large as 320 meV, indicating large potential fluctuations on the sample surface. These fluctuations are caused by the inhomogeneous distribution of the charged clusters. Since we neither know which clusters are charged nor the position of the compensating acceptors, we cannot calculate the potential landscape exactly. However, a good estimate is obtained. Therefore, we take the 50% clusters with the lower Coulomb gap to be charged, giving the known 50% charging probability. To the resulting charge distribution, we add the compensating charged acceptors randomly. Then, we fold the deduced 3D potential with the shape of the first 2DES subband in the  $z$  direction.<sup>5,11</sup> Figure 1(f) shows the resulting 2DES potential. It fluctuates by about 100 meV (Ref. 12) on a length scale of 40 nm, and exhibits two partly connected valleys, from which the one marked QD contains confined states as shown below.

We ignore the potential fluctuations for the moment and calculate the subband energies  $E_n$  of the 2DES. Therefore, we solve the one-dimensional Poisson and Schrödinger equations using the measured surface  $E_F$  shift (500 meV) as the only input parameter.<sup>11,13</sup> We find  $E_0 - E_F = 40$  meV,  $E_1 - E_F = 150$  meV, and  $E_2 - E_F = 220$  meV, i.e., all subbands are empty. Indeed, we find curves with steps close to the calculated  $E_n$ , if we average  $dI/dV$  curves over selected areas of the sample, i.e., within about 40% of the total area. Figure 1(d) shows such a curve, which is similarly found in

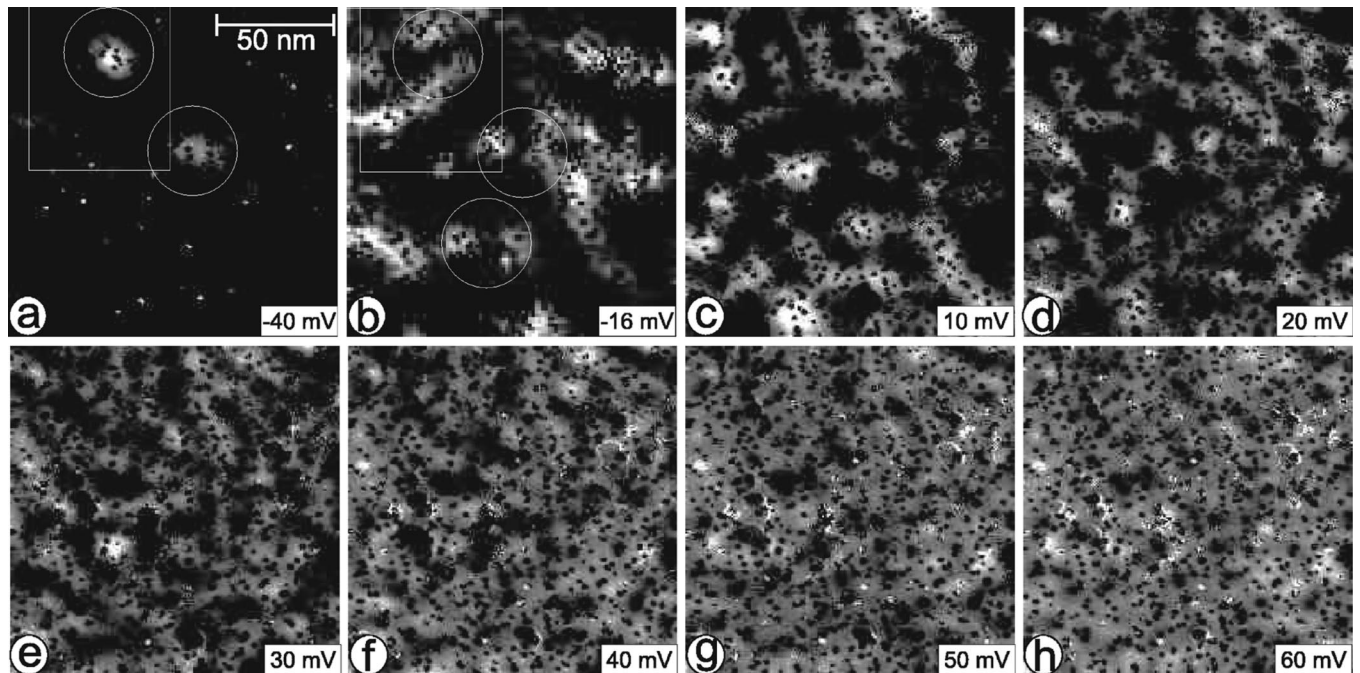


FIG. 3. (a)–(h)  $dI/dV$  images of a larger 2DES region recorded at different  $V$  as indicated,  $I_{stab}=700$  pA,  $V_{stab}=430$  mV, and  $V_{mod}=5$  mV; all images show exactly the same sample region; the potential area of Fig. 1(f) is marked as a rectangle in (a) and (b); the circles in (b) mark three  $p$  states, identified by finding the corresponding  $s$  state at a lower voltage.

the flat potential area marked as 2D in Fig. 1(f). The steps are at about 30, 140, and 220 mV, in good agreement with expectations. However, already the photoemission data revealed that the 2DES is occupied by  $1 \pm 0.7 \times 10^{11}$  electrons/cm<sup>2</sup>.<sup>5</sup> These occupied states are located in most of the remaining sample areas [55% (Ref. 14)]. Figure 1(e) shows a  $dI/dV$  curve of an area exhibiting two peaks below  $E_F$ . Note that the partial appearance of the peaks and the fact that they do not shift in energy with position excludes that the peaks originate from the tip-induced quantum dot.<sup>8</sup> In contrast, the peaks represent completely confined states of the sample as evidenced in Fig. 2. Corresponding  $dI/dV$  curves are displayed in Figs. 2(a) and 2(d), and LDOS maps taken close to the peak voltages are shown in Figs. 2(b), 2(c), 2(e), and 2(f). One finds that the lower peaks correspond to a rather symmetric  $s$ -like LDOS, while the upper peaks show two lobes as known from  $p$  states. Obviously, the occupied states of the 2DES are confined. This confinement is caused by the potential valleys of the sample as demonstrated in Figs. 3(a) and 3(b). The potential region of Fig. 1(f) is marked and  $s$ - and  $p$ -like states appear in the upper potential valley. Moreover, the  $p$ -like state is elongated in the direction of the largest valley extension. Note that the states deviate from ideal  $s$  and  $p$  shapes due to the irregular shape of the valleys. Two peaks in the same valley are on average separated by  $\Delta E = 18 \pm 5$  meV; the corresponding  $s$  states have a full width at half maximum of  $d_s = 19 \pm 3$  nm and the lobe maxima of the  $p$  states are  $\Delta_p = 26 \pm 7$  nm apart. This is nicely reproduced, assuming a parabolic quantum dot of  $0.12$  meV/nm<sup>2</sup> curvature ( $\Delta E = 18$  meV,  $d_s = 20$  nm,  $\Delta_p = 24$  nm). Indeed, a curvature of about  $0.1$  meV/nm<sup>2</sup> is found in the upper valley of Fig. 1(f).

Of course, only a few of the valleys contain two states below  $E_F$ . The majority exhibit only one peak with an  $s$ -like appearance. We found that 15% of the valleys contain two states and 85% only one state. To determine the total occupancy of the 2DES, we simply count all  $s$  and  $p$  states twice for spin degeneracy, which results in  $1.8 \pm 0.3 \times 10^{11}$  electrons/cm<sup>2</sup>, in reasonable agreement with the photoemission results.<sup>5</sup>

A 2DES consisting of separated electron droplets is known to be insulating at low temperature.<sup>15</sup> Ignoring weak localization, one expects a density driven transition to conduction usually described within percolation theory.<sup>2</sup> For symmetric potential landscapes the classical percolation appears at the mean of the potential,<sup>1</sup> which is the subband energy calculated within the one-dimensional model. Thus, we expect percolation around 40 meV. Figure 3 shows larger LDOS maps obtained at different  $V$ 's. At low  $V$ , two  $s$  states are visible in Fig. 3(a) and three  $p$  states, identified by finding a corresponding  $s$  state at lower energy, are encircled in Fig. 3(b). At higher  $V$ , an increasing part of the surface gets covered with the LDOS. In a simplified approach, one would identify the percolation with the energy where the bright areas form a percolating path, i.e., at 20 mV. However, since the energy resolution is finite, this apparent percolation can result from partly overlapping localized states at different energies. Thus, we cannot determine the percolation threshold by standard analysis.<sup>1</sup> Instead, we find a strong reduction

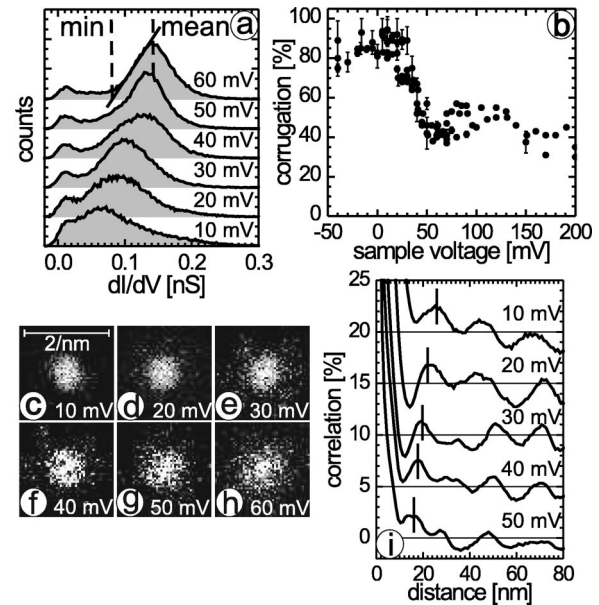


FIG. 4. (a) Histograms of  $dI/dV$  values obtained within the images of Fig. 3 (curves offset for clarity); the larger peak in each curve corresponds to the 2DES region; dashed lines on the (60 mV) curve indicate minimum and mean values used to determine corrugation  $C$  (see the text). (b) Obtained corrugation  $C$  as a function of  $V$  (error bars indicated). (c)–(h) Fourier transforms of  $dI/dV$  images with length bars in units of  $k = 2\pi/\lambda$ . (i) Spatial correlation function of  $dI/dV$  images; curves are offset by the distance of horizontal lines; wavelengths corresponding to squared wave functions, as expected from the InAs dispersion, are marked by vertical lines.

of corrugation close to the expected threshold of 40 mV. This is demonstrated in Fig. 4. Figure 4(a) shows histograms of the  $dI/dV$  values. Each histogram exhibits two peaks, whose origin is found by displaying only the LDOS of one peak. This reveals that the lower peak is caused by the Co clusters, which, due to the Coulomb blockade, show  $dI/dV = 0$ . The upper peak represents the 2DES, and its minimum (min) and mean  $dI/dV$  value are determined as marked in Fig. 4(a). Then, the corrugation strength of the 2DES LDOS is deduced as  $C = (\text{mean} - \text{min})/\text{mean}$ .<sup>6</sup> It is plotted in Fig. 4(b) and drops rather sharply around 35 mV.

A drop in corrugation is indeed expected at percolation. Below percolation, the confined states are separated by areas of zero LDOS, resulting in  $C \approx 100\%$  as observed. In contrast, the extended states above percolation overlap. A strongly simplified model explains the resulting reduction in  $C$ . We divide the image area  $A$  of Fig. 3 into 300 boxes of width of about half LDOS wavelength. This is 10 nm, as can be deduced from Fig. 4(i) (see below). Then, we calculate the number of contributing states  $N$  from the known 2DES density of states  $D$  (Ref. 14) and the experimental energy resolution  $\delta E \approx 2.5 V_{mod}$  giving  $N = D \times \delta E \times A = 30$  (Ref. 6). Finally, we randomly put a zero or a one into each box for each wave function, which represent maxima and minima of the wave functions. The probability to obtain a sum of  $n$  in a box is  $P(n) = \binom{30}{n} \times 0.5^{30}$ . To find a minimum value  $n$  within an image,  $n$  should occur at least in one box, i.e.,  $P(n) \geq 1/300$ . This is the case for  $n = 8$ , but not for  $n$

$=7$ . We get  $C=(15-8)/15=0.47$ , in agreement with experiment. Thus, we conclude that the drop in  $C$  is a characteristic property of percolation.

An interesting question is, whether classical percolation is an adequate model to describe the transition. It assumes that electrons are small enough to fill into the available space given by the potential landscape. Since rearrangements in the electron density are typically governed by the Fermi wavelength,<sup>16</sup> this assumption might be wrong. However, in a strong disorder potential, a significant mixing of electron waves takes place.<sup>17</sup> Thus, the Fermi wavelength is not a well defined quantity. The mixing becomes evident from Fourier transforms (FTs) representing the  $k$ -space distribution of the LDOS as shown in Figs. 4(c)–4(h). The FT of a clean system would exhibit rings growing in radius with energy, as is indeed observed for a less disordered 2DES.<sup>6</sup> Here, we find instead a filled circle with a radius barely depending on energy. We conclude that the mixing induced by the strong disorder suppresses dominating wavelengths. In other words, the concept of a Fermi wavelength breaks down. A small remainder of the dominating wave length is found in the spatial correlation functions of the LDOS shown

in Fig. 4(i). The expected dispersion wavelength is indicated and one observes a tiny peak of 1.5% strength at this distance and further peaks at multiple distances. Obviously, there is a small tendency of the LDOS to prefer next maxima in the distance of the expected wavelength. However, we do not think that this small tendency will influence the percolation significantly. We conclude that wavelength effects are of minor importance around percolation, implying that a classical description might be sufficient.

In summary, we analyzed the LDOS of a strongly disordered 2DES measured by scanning tunneling spectroscopy. At low energies we find quantized states of  $s$ - and  $p$ -like character confined in individual valleys of the potential landscape. At higher energies we observe percolation indicated by a spreading of LDOS across the whole 2DES area and a significant decrease in corrugation strength. Around the percolation transition, a dominating wavelength is barely present implying, that the system behaves rather classically.

We thank A. Wachowiak for helpful discussions and acknowledge financial support from Wi 1277/15-2, SFB 508 and Graduiertenkolleg ‘‘Physik nanostrukturierter Festkorper’’ of the DFG.

<sup>1</sup>D. Stauffer, *Introduction to Percolation Theory* (Taylor & Francis, London, 1985); J. Ziman, *Models of Disorder—the Theoretical Physics of Homogeneously Disordered Systems* (Cambridge University Press, Cambridge, 1979); S. Kirkpatrick, *Rev. Mod. Phys.* **45**, 574 (1973); M.B. Isichenko, *ibid.* **64**, 961 (1992).

<sup>2</sup>Y. Meir *et al.*, *Phys. Rev. Lett.* **83**, 3506 (1999); *Phys. Rev. B* **61**, 16470 (2000); **63**, 073108 (2001); S. He *et al.*, *Phys. Rev. Lett.* **80**, 3324 (1998).

<sup>3</sup>K.M. Lang *et al.*, *Nature (London)* **415**, 412 (2002); H.H. Wen *et al.*, *Europhys. Lett.* **57**, 260 (2002); J.C. Phillips, *Philos. Mag. B* **82**, 783 (2002); T. Cren *et al.*, *Europhys. Lett.* **54**, 84 (2001).

<sup>4</sup>M. Fath *et al.*, *Science* **285**, 1540 (1999); J.M. De Teresa *et al.*, *Nature (London)* **386**, 256 (1997); H.L. Liu *et al.*, *Phys. Rev. B* **58**, R10115 (1998).

<sup>5</sup>M. Morgenstern *et al.*, *Phys. Rev. B* **65**, 155325 (2002).

<sup>6</sup>M. Morgenstern *et al.*, *Phys. Rev. Lett.* **89**, 136806 (2002).

<sup>7</sup>Chr. Wittneven *et al.*, *Rev. Sci. Instrum.* **68**, 3806 (1997).

<sup>8</sup>R. Dombrowski *et al.*, *Phys. Rev. B* **59**, 8043 (1999).

<sup>9</sup>M. Morgenstern *et al.*, *J. Electron Spectrosc. Relat. Phenom.* **109**, 127 (2000).

<sup>10</sup>J. Tersoff *et al.*, *Phys. Rev. Lett.* **50**, 1998 (1983); *Phys. Rev. B* **31**, 805 (1985).

<sup>11</sup>T. Ando *et al.*, *Rev. Mod. Phys.* **54**, 437 (1982).

<sup>12</sup>The lower fluctuation with respect to the one deduced from the Coulomb gap centers is a consequence of the distance of the 2DES from the surface.

<sup>13</sup>U. Merkt *et al.*, *Phys. Rev. B* **35**, 2460 (1987).

<sup>14</sup>The missing 5% show only a confined state above  $E_F$ .

<sup>15</sup>B. I. Shlovskii *et al.*, *Electronic Properties of Semiconductors* (Springer, Heidelberg, 1984).

<sup>16</sup>J. Friedel, *Philos. Mag.* **43**, 153 (1952).

<sup>17</sup>C. Metzner *et al.*, *Phys. Rev. B* **58**, 7188 (1998); M. Hofmann *et al.*, *ibid.* **64**, 245321 (2001); J. Shi *et al.*, *Phys. Rev. Lett.* **88**, 086401 (2002).